



Abschlussbericht 29. November 2012

Spray Combustion Chamber

Weiterentwicklung eines Referenzexperiments
("Spray Combustion Chamber") in Bezug auf die
Optimierung des Verbrennungssystems von
Grossdieselmotoren

Auftraggeber:

Bundesamt für Energie BFE
Forschungsprogramm Verbrennung
CH-3003 Bern
www.bfe.admin.ch

Kofinanzierung:

Wärtsilä Switzerland Ltd, CH-8401 Winterthur
EU FP-7

Auftragnehmer:

Wärtsilä Switzerland Ltd
Zürcherstrasse 12
CH-8401 Winterthur
www.wartsila.com

Autoren:

Andreas Schmid, Wärtsilä Switzerland Ltd, andreas.schmid@wartsila.com
Beat von Rotz, Wärtsilä Switzerland Ltd, beat.vonrotz@wartsila.com
Kai Herrmann, Wärtsilä Switzerland Ltd, kai.herrmann@wartsila.com
German Weisser, Wärtsilä Switzerland Ltd, german.weisser@wartsila.com

BFE-Bereichsleiter: Sandra Hermle

BFE-Programmleiter: Stephan Renz

BFE-Vertrags- und Projektnummer: 154269 / 103241

Für den Inhalt und die Schlussfolgerungen sind ausschliesslich die Autoren dieses Berichts verantwortlich.

Table of Contents

Table of Contents	3
Abstract	4
Introduction.....	6
Further development of the test facility.....	8
Heavy Fuel Oil (HFO) injection system	8
Adaptation for testing production injector configurations	9
Enhancement of optical accessibility.....	9
Concept for allowing tests with only small quantities of fuel	10
Application and further development of measurement techniques	12
Shadow-imaging technique optimization.....	12
MIE-scattering technique application	12
OH*-chemiluminescence application.....	13
OH* probe application.....	14
Phase Doppler Anemometry (PDA) application	15
Results.....	16
Phenomenological aspects	16
Reference data generation with light fuel oil (LFO)	16
Assessment of fuel impact.....	20
Ignition behaviour investigations	21
Determination of droplet size distribution	23
Extended application: Investigation of lubrication oil injection	25
Conclusions and Outlook	27
National Collaboration.....	28
International Collaboration	28
References	29

Abstract

The purpose of the project has been the further development and utilisation of a novel experimental test facility (Spray Combustion Chamber – SCC) with optical accessibility, which represents the combustion chamber of a 2-stroke marine diesel engine and allows the investigation of in-cylinder processes at realistic conditions. This involves the enhancement of the experimental setup (also in view of a potential use in the context of product development projects) as well as the further development of existing and the application of new technologies with the ultimate target of generating a comprehensive set of reference data, which can be used for the validation and improvement of CFD tools.

One main topic has been the ability to operate the SCC on different fuels, including customary marine fuel types. In this respect, the operational flexibility and efficiency have been considerably enhanced by implementing an additional fuel injection system for heavy fuel oil. A next step is already in progress, which shall enable the investigation of even very small quantities of either model or alternative fuels or even of samples of fuels of different quality actually used on board vessels.

Another major achievement has been the redesign of the covers for improved optical accessibility, which clearly reduces the efforts during measurement campaigns for observing the spray along its full penetration. On the one hand, a significantly smaller number of measurement locations (window positions) is required. On the other hand, also the change of window position can be realised more efficiently as the need for rotating the covers is almost limited to a minimum.

Following the optimisation of the experimental setup for shadow-imaging investigations, the range of measurement techniques has been extended by applying Mie-scattering, OH*-chemiluminescence and Phase Doppler Anemometry. The applicability of all these techniques has been demonstrated and first results have been obtained with respect to droplet sizes and velocities as well as ignition and combustion behaviour.

These technologies will also be applied in the future for complementing the reference data base for spray propagation, which has been established in the course of the present project and consists in relevant characteristics such as penetration and spray angles for a whole range of conditions. The variations considered include the most important parameters for (single) light fuel oil sprays such as chamber pressure and temperature, injector orifice size, spray orientation with respect to the swirl, swirl intensity or injection pressure. Further investigations into fuel quality effects will be performed in order to extend the range of applicability of this comprehensive reference data set, which is already now extensively used for the validation of CFD modelling approaches.

Regarding more product development related investigations, the potential of the SCC has been confirmed by realising a special configuration allowing the observation of sprays from actual production injectors. Moreover, its versatility has been demonstrated by using it for studying lubricant oil injection at conditions relevant for lubrication systems on large two-stroke engines.

The investigations confirm the potential of the experimental test facility for studying spray and combustion processes at conditions relevant to large marine diesel engine combustion and extend the information on spray characteristics at such conditions.

All in all, the Spray Combustion Chamber has clearly demonstrated its value: It has proven its robustness and can be operated at high levels of reliability. It allows generating data, which are characterised by outstanding reproducibility and very high quality. The data processing, which has been specifically devised, enables the fast and efficient analysis of the raw data obtained in order to derive relevant scientific conclusions. Its unique features and high versatility make it a very powerful and invaluable tool both for fundamental research into spray and combustion processes and for enhancing product development by assessing the performance of new components and systems that can be applied to it. Its availability to the Swiss research community must be seen as a major asset in terms of the competitive position of the contributing partners.

Project Objectives

In view of the global ecological changes as well as the continuing environmental challenges on a more regional or local level, the transport sector is one of the focus areas in order to achieve further emissions reductions by means of new technologies and concepts. This also refers to shipping, which accounts for up to 90% of the worldwide transportation of cargo, while contributing less than 5% to the consumption of fossil fuels and less than 3% of the global CO₂ emissions. In contrast, the global share of nitrogen oxide and sulphur oxide emissions is considerably higher and trendwise even increasing due to higher transport volumes and the effect of the substantial reductions associated with the introduction of advanced concepts as a consequence of increasingly more stringent regulations in the other sectors.

Therefore, the marine sector is also subject to more and more strict emissions limits. For example, the NO_x limit for engines with a rated speed below 130 rpm has been lowered from 17 g/kWh to 14.4 g/kWh by 2011 and will be substantially further reduced to 3.4 g/kWh (applicable within so-called Emission Control Areas (ECA)) by 2016. In parallel, the sulphur oxide as well as the particulate matter emissions shall be reduced considerably by gradually further constraining the maximum allowable fuel sulphur content, both globally and inside ECAs – or by using alternative technologies yielding corresponding emission levels. Moreover, measures are taken in order to even further reduce the CO₂ emissions from shipping from their already very low levels.

In order to be able to cope with the associated challenges towards the development of marine diesel engines, the use of more advanced simulation models must be considered indispensable. The application of these tools shall complement (and, ultimately, even partly replace) the comprehensive measurements on specific test engines for optimising the combustion and emissions behaviour and hence general performance of marine diesel engines. The availability of fundamental reference data is an absolute prerequisite for the systematic application and improvement of existing calculation models, respectively for the further development of such "Computational Fluid Dynamics" (CFD) simulations tools for the optimization of combustion systems.

Therefore, a novel experimental test facility – representative of the combustion system of a 2-stroke marine diesel engine at typical operation conditions – has been developed [1] within the I.P. HERCULES-Project [2] and with financial support of the Swiss Federal Office of Energy [3]. The so-called Spray Combustion Chamber (SCC) has subsequently been used in the follow-up projects HERCULES-B ([4], 2008-2011) and HERCULES-C ([5], since 2012), mainly for the investigation of spray and combustion processes in order to improve the general understanding of in-cylinder processes and generate reference data for simulation model improvement and validation.

Beyond these projects, an essential objective has been the further development of the existing test facility per se towards a component test bench allowing also "product related research". This refers to investigations of fuel influence (ignition behaviour) and the use (behaviour) of other (alternative) fuels. Furthermore, the test facility should be completed with novel components or configurations (e.g. covers) and also allow development tests of new product components (e.g. injection nozzles). Another important issue is the application of optical measurement techniques at difficult conditions, also related to their applicability. This can again be expected to contribute to the better understanding of the key phenomena and the extension of the reference data base.

Based on these considerations, three specific targets could be identified

- Enhancement of the experimental setup: The design was extensively tested. Based on this experience selected parts have been improved and/or upgraded.
- Further development of existing and application of new measurement technologies: The size of the SCC as well as its temperature and pressure conditions made it necessary to adapt standard measurement technologies.
- Acquisition of reference data: In extensive measurement series various aspects of the combustion of marine diesel sprays have been investigated.

Introduction

An overview of the Spray Combustion Chamber (SCC) test facility [1], which was developed in the context of the I.P. HERCULES project [2] and with financial support of the Swiss Federal Office of Energy [3] is given in Figure 1:

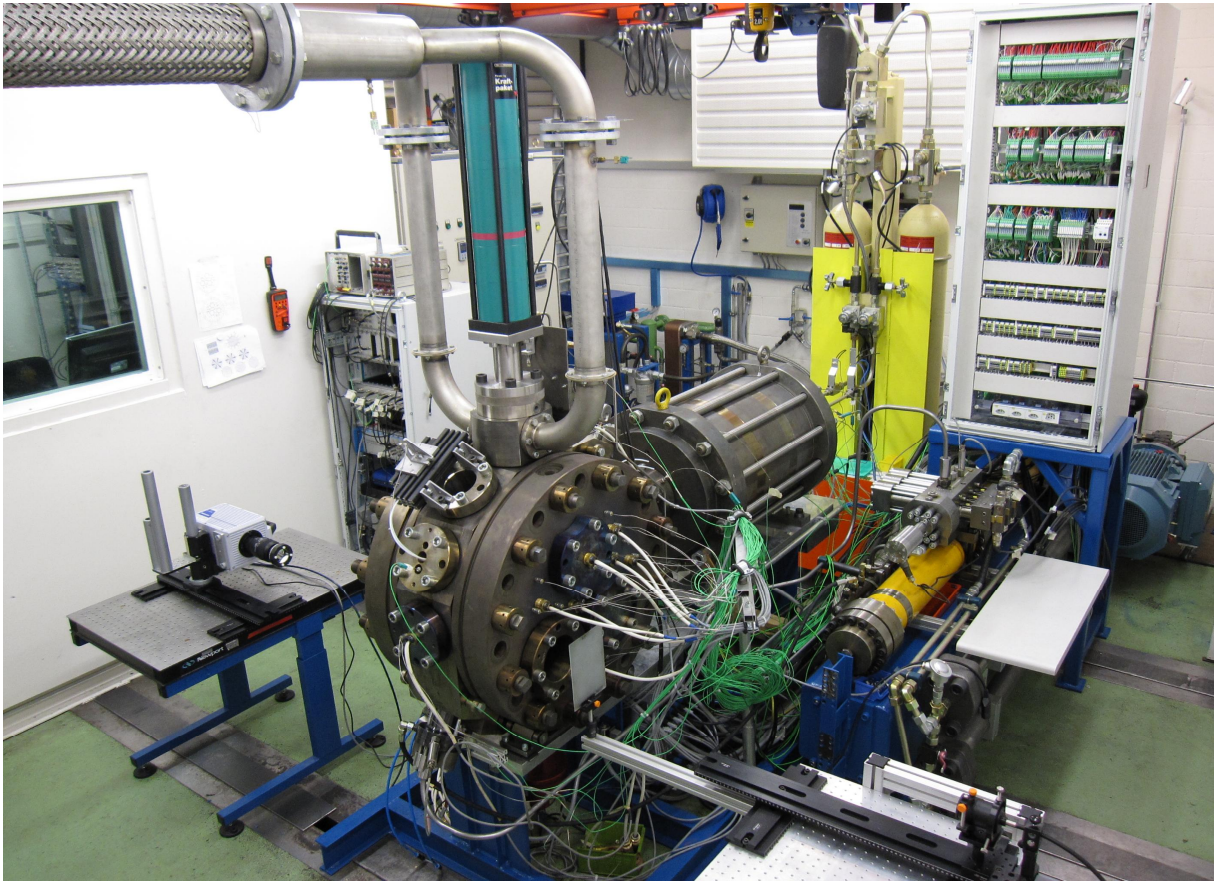


Figure 1: Spray Combustion Chamber test facility setup.

Besides the actual constant volume combustion chamber ($\text{\O}500 \times 150 \text{ mm}$) visible in the front part, it includes also various subsystems, which allow achieving relevant conditions inside the chamber at start of injection: Gas pressure and temperature are provided by a pressure vessel/heat regenerating system and a swirl flow pattern is generated by introducing the gas to the chamber via inclined intake channels. The design includes comprehensive options for granting optical access and involves multiple injector arrangement variants. The common rail injection system is largely similar to systems in operation on current engine designs.

The performance of the test facility was assessed in the context of initial validation tests and its compliance with the requirement specification confirmed: The left diagram in Figure 2 shows exemplary pressure and temperature data of a typical operation (filling) process [6] (accumulator pressure of 340 bar, valve actuating time of 750 ms, regenerator inner core temperature of $950 \text{ }^\circ\text{C}$). The pressure p_{inlet} is measured at a position close to the inlet of the regenerator right after the fast actuating valves of the pressure accumulator bottles. T_{flange} illustrates the regenerator exit, respectively Spray Combustion Chamber inlet temperature at a sensor position in the flange in between. The SCC condition acquiring sensors (p_{SCC} , T_{SCC}) are located opposite to the swirl producing intake channels.

The pressure and temperature histories illustrate the working principle of the setup: Following the opening of the fast actuating valves, p_{inlet} rises sharply, whereas p_{SCC} increases much slower due to the high pressure loss in the regenerator. Both reach their maximum some time after the closing of the valves, followed by a subsequent gradual decrease as a consequence of the heat losses. These are also clearly visible in the temperature histories, where

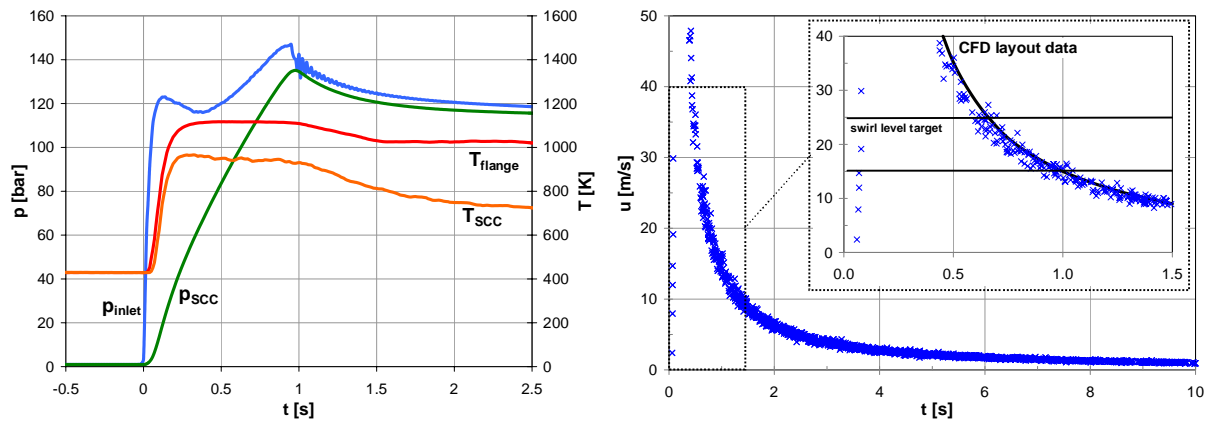


Figure 2: Pressure, temperature (left) and swirl (right) evolution during a sample filling process

also the effect of the distance from the regenerator can be seen in the difference of the two signals T_{flange} and T_{SCC} .

Flow investigations were performed by means of a common LDV system (seeding silver-coated hollow glass spheres) specified for velocity measurements up to 150 m/s. The results obtained at a radial position of the measurement point on the centre plane at 200 mm from the chamber axis are shown in the right diagram in Figure 2.

The flow measurement results are consistent with the data obtained in extensive CFD simulations performed as part of the development [7] and thus confirm the selection of the inlet port geometry, which was made on that basis. The observed swirl decay characteristic seems to be independent of the pressure and temperature levels considered due to the presence of overcritical conditions in the gas supply system at those levels. The target velocity range is reached at about 0.75 s. Hence, considering the pressure and temperature levels present in the chamber by that time, one can state that the targeted levels of 120 bar and more than 900 K have been reached. These conditions can then be adjusted by varying the accumulator pressure and/or the opening valve time and the regenerator core temperature.

Further development of the test facility

During the validation and initial application as well as the extensive use of the installation ever since, a lot of experience related to the operation of the SCC itself as well as to the application of several measurement techniques has been accumulated. This has triggered the identification of various options for making the setup even more efficient, more flexible and for further improving the quality of the acquired data. Additionally, the test facility was equipped with new features which made it possible to investigate product-related issues and to proactively support different fields in two-stroke research and development here in Switzerland.

Heavy Fuel Oil (HFO) injection system

A very important step towards completion of the entire experimental test facility has been the extension of the fuel system in order to facilitate the application of different fuels. As the volume of the complete injection system is relatively large, a change of fuel would normally involve draining the one fuel completely, purging the complete system and refilling it with the other fuel. In particular, the envisaged tests with Heavy Fuel Oil (HFO, which is the customary fuel in marine engine applications), in view of its particular properties and characteristics (f.i. that its temperature has to be kept above a certain temperature in order to allow the pressurizing and injection into the combustion chamber), would be associated with non-negligible efforts. Therefore, the decision has been made to introduce a second, independent system for such fuel types, thereby using synergies with existing infrastructure, e.g. by connecting it to the existing HFO supply and conditioning system at the Diesel Technology Center. It has also been possible to make use of an existing HFO aggregate, formerly used for fuel pump tests, which was upgraded and connected to a new fuel rail, from where the fuel is metered via the associated Injection Control Unit (ICU) to the injector(s) of the SCC (Figure 3). This system is now equipped with appropriate heating capacity (from 8 kW to 50 kW) and sufficient insulation solutions. In addition, a newly implemented viscosimeter provides online information about the density and viscosity such that the actual fuel properties can be recorded and, ultimately, even controlled (by heating or cooling) in order to comply with specific requirements. Furthermore, the existing main control system was expanded in order to accommodate this alternative injection system and the associated signals and enable the automatic operation of this heavy fuel oil aggregate.



Figure 3: Lower left: Heavy Fuel Oil-pump with viscosity measurement as well as heating device.
Middle: HFO Common Rail (vapour heated and isolated) with ICU.
Upper right: HFO piping to the injector.

Adaptation for testing production injector configurations

The so-called "injector-in-dummy" (IID) concept shown in Figure 4 enables an assembly of the injector through the cover (similar to the engine design). This provides further flexibility related to investigations of commercial marine diesel injector nozzle layouts and with regard to optical access for the simultaneous spray observation through a front and a side window. The piping from the ICU on the fuel rail to the injector includes a distribution block which is axis-symmetric to the revolvable cover. This offers the possibility of adjusting the desired measurement spray location directly by rotating the cover.

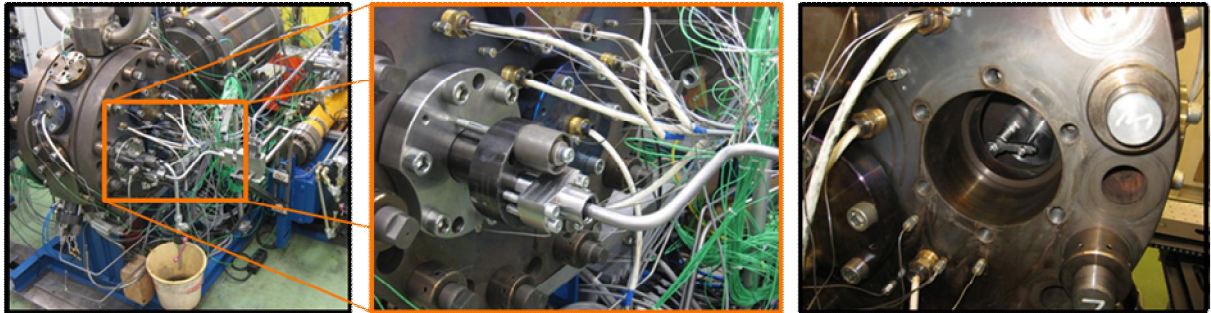


Figure 4: Injector in Dummy (IID) concept.

Figure 4 (right) shows an extension of the IID setup with an additional design of the dummy (as injector holder) which enables a fuel discharge out of the combustion chamber. The discharging high pressure pipe is equipped with a corresponding fuel gate valve (just above the bucket in the left image of Figure 4) in order to provide leak-tightness of the spray combustion chamber during the process gas filling, the injection and the combustion phase. Additionally, the front view of the fuel discharging design is shown in Figure 4 (right). It consists of a special (single-hole) injection nozzle where a part of the provided fuel is lead away from the spray combustion chamber through a side branch connected to the fuel discharging port mounted on the dummy front plane closing the chamber.

Enhancement of optical accessibility

The windows of the SCC allow an optical access of about 100 mm diameter. As was known by the time of the development of the SCC already (and as various investigations showed, since), this is not enough to visualise the spray of a marine 2-stroke diesel engine (Figure 5)

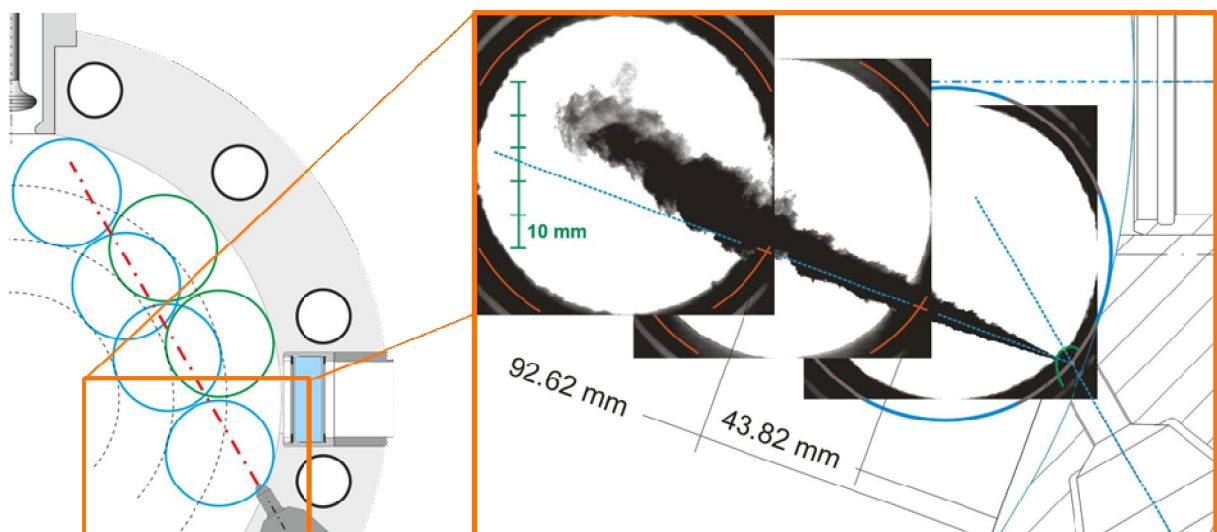


Figure 5: Measurement of spray penetration over three Window positions (right) and possible combination of window positions due to rotation of the covers (left side)

for a sufficiently long period after start of injection. Therefore, the covers of the SCC were designed in such a way that they can be rotated. This allows covering different circumferential locations, while the positions of the individual window drillings allow covering most of the combustion chamber. As can be seen in Figure 5 (left side), some positions can't entirely be covered by the windows, which results in loss of information. Moreover, the rotation of the covers is very time consuming and increases the cycle load on the bolts to fix the covers, as these bolts are under high pretension and have to be loosened and tightened again each time the covers have to be rotated. These facts inspired the reconsideration of the system and the redesign of the covers. The new design contains bigger windows (optical diameter 150 mm) and a new window holder with eccentric window position. Figure 6 (2 images on the outer left) shows the drawing of the new window holders with the eccentric position of the 150 mm windows and a 3D-assembly with the new covers and windows for the Finite Element Method (FEM) simulation, together with the new cover and window holder as manufactured in comparison to the old cover with two dummies mounted.

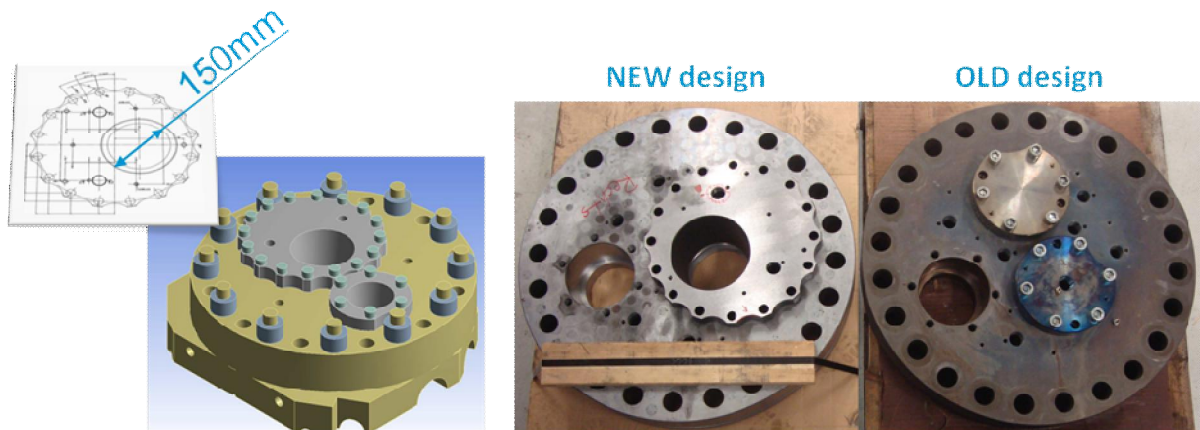


Figure 6: Design of the new eccentric window holders with 3D Model of the new covers for FEM analysis (left) and comparison between old and new cover design (right)

The bigger window diameter allows the observation of a wider area of the spray, which reduces the effort for turning the covers. At the same time, the eccentricity of the window holder offers the possibility of adjusting the window position within a certain range. The rotation of the window holder is much faster than the rotation of the covers. The rotational degree of freedom of the covers persists; however, the bigger window diameter in combination with the possibility to change its position via the eccentricity of the window holders allows covering a larger portion of the spray without the necessity of turning the covers. With the new installations, the flexibility of the SCC and the efficiency in its operation have been clearly further improved. In principle, the measurement locations for all reactive investigations can now be adjusted simply by rotating the eccentric holder containing the larger window.

Concept for allowing tests with only small quantities of fuel

The HFO system presented earlier is a very good and valuable tool for the investigation of differences between typical heavy and light fuel oil spray behaviour. However, in case measurement series with additional fuel types are envisaged, this remains to be associated with substantial efforts and cost as one of the rail systems including pump and tank system would have to be drained, purged and refilled with the fuel to be tested. Specifically when targeting f.i. single-component model fuels or particular fuel qualities used out in the field, this must be considered prohibitive. Another aspect is the sensitivity of the ICU in terms of lubricity properties of the fuel: Single component fuels as they are needed in reference experiments for CFD comparisons often show very poor lubricity properties. Therefore, it was decided to build a media separator. The idea is to use the LFO (or HFO) fuel system to generate the injection pressure. The media separator (see schematic drawing in Figure 7) is located in the fuel line between ICU and injector and transfers the pressure to any kind of fuel. As a consequence, only relatively small samples of fuel are needed.

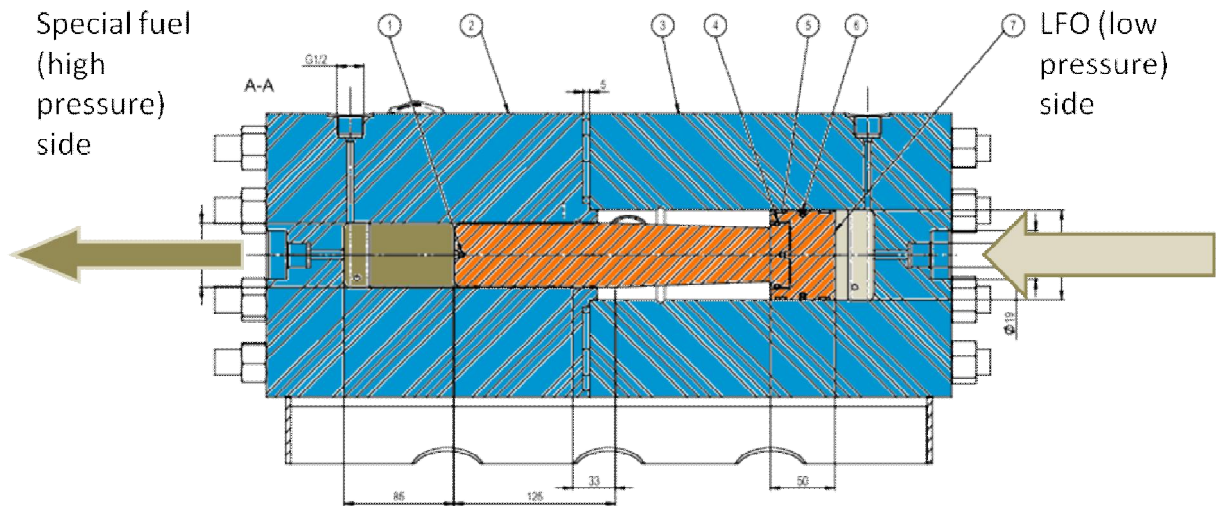


Figure 7: Sectional view of the media separator with the low pressure/LFO side on the right and the high pressure side on the right.

An additional design feature of the media separator is associated with the fact that the area on the LFO side is double the area on the other side of the piston. This gives a pressure ratio of 2:1 between the special injection pressure and the LFO side, which extends the operation range by increasing the maximum injection pressure from the 1200 bar design limit of the rail used up to 2400 bar. As future combustion systems are expected to require higher injection pressure, this feature is seen as an important enhancement in order to allow the proactive investigation of the effect of those higher pressures on sprays and combustion.

Application and further development of measurement techniques

The size of the SCC in combination with the in-cylinder conditions at which marine diesel engines operate, drastically restricts the choice of applicable measurement techniques. Most of the investigation methods that are used at the SCC had to be adapted in order to allow the measurement in the given environment. Some of these enhanced techniques have been presented at conferences (e.g. [8]) while others have even been taken into the portfolio of known providers of measurement techniques [9]. Today, the SCC is equipped with a variety of measurement techniques allowing the investigation of several spray and combustion related characteristics, which completes the test facility and makes it a powerful tool in the investigation of marine diesel spray and combustion.

Shadow-imaging technique optimization

In a first stage, the spray propagation inside the chamber has been visualized by means of the "Shadow-imaging" (background illumination) method [10] using various light sources (arc or QTH-lamp) and a high-speed (20kHz / 512x512 pixel) CMOS-camera. The illumination and observation windows were mounted in the outer position for obtaining optical access to the region directly adjacent to the injector tip in order to allow the observation of the initial spray propagation. Reactive investigations have been performed for assessing the ignition behaviour at various chamber conditions. The upper sequence of Figure 8 shows a series of images illustrating the ignition process of a two spray configuration at high pressure and

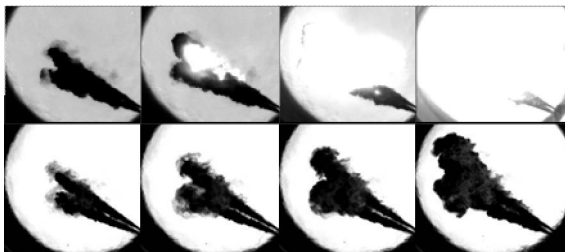


Figure 8: Shadow-imaging measurements of the spray evolution with a regular arc-lamp (upper sequence) and the improved laser background light source (lower sequence).

temperature conditions in the spray combustion chamber at start of combustion. In this case, the ignition is occurring within the observation area at a position rather on the lee side of the sprays and combustion is then spreading both towards their tips and the injector. These image series are based on a standard background illumination with an arc lamp light source. Obviously, the flame luminescence is dominating the background illumination once the combustion is fully developed. The CMOS-sensor of the camera gets overexposed and this clearly represents a problem for the visualization of the spray in the late phase. A solution for this problem has been found in applying an alternative illumination concept, consisting in a pulsed diode laser light source combined with a high-speed CMOS-camera, where the synchronization can be adjusted according to the injection start. Additionally, a flame light blocking filter is placed in front of the camera such that, due to an extremely short laser pulse (50 ns) within a very short exposure time (1 μ s) of the camera, an increase of the recordings' signal-to-noise ratio can be achieved. As a consequence, considerably "sharper" images are obtained and it is possible to continue observation of sprays even after ignition has taken place. This is clearly demonstrated in the lower sequence of Figure 8, which refers to the same configuration and conditions as in the upper and where the propagation of the sprays remains clearly detectable well beyond their ignition.

ode laser light source combined with a high-speed CMOS-camera, where the synchronization can be adjusted according to the injection start. Additionally, a flame light blocking filter is placed in front of the camera such that, due to an extremely short laser pulse (50 ns) within a very short exposure time (1 μ s) of the camera, an increase of the recordings' signal-to-noise ratio can be achieved. As a consequence, considerably "sharper" images are obtained and it is possible to continue observation of sprays even after ignition has taken place. This is clearly demonstrated in the lower sequence of Figure 8, which refers to the same configuration and conditions as in the upper and where the propagation of the sprays remains clearly detectable well beyond their ignition.

MIE-scattering technique application

The scattering of electromagnetic radiation by spherical particles is covered by different scattering theories depending on the particle size relative to the light wavelength – the term "Mie-scattering" is commonly used for scattering particles with diameters $> 10\%$ of the light wavelength. In combustion diagnostics, especially (fuel) sprays and droplets fall into this size

range. The scattered light intensity is proportional to the droplet concentration and the square of the droplet diameter but no quantitative analysis (droplet sizes, droplet densities) is possible. Nevertheless, the technique is able to deliver a lot of information about the spray, such as penetration, cone angle, injector quality (reproducibility, needle bouncing), and the detection of the effective (hydraulic) injection start/end. Mie-scattering basically is an inverted shadow-imaging method, where no illuminated background is required for the object under investigation.

Figure 9 (left) shows the Mie-scattering setup at the spray combustion chamber. In order to have sufficient illumination power combined with a high laser pulse frequency, a so-called Nd:YLF laser was employed. It provides a 20 kHz repetition rate with very short laser pulses (ns) of sufficient energy, which can be synchronized with the exposure time of the high-speed camera operating at the same frequency. The laser beam itself has to be aligned such that its path is adjusted to 50% beam splitters dividing it into two beams which are expanded and shaped by a specific lens system (Figure 9 right) to illuminate (around the camera) the desired observation area through the front window of the spray combustion chamber.

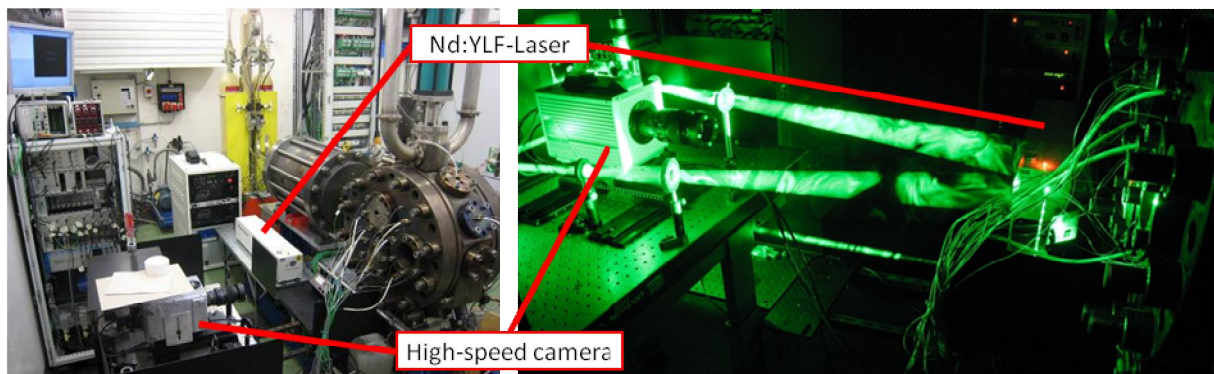


Figure 9: Nd:YLF-laser setup (left) with laser beam alignment (lens design) for the front illumination to allow spray MIE-scattering recordings with the high-speed camera (right).

OH^{*}-chemiluminescence application

To gain information about the ignition of the fuel, the observation of OH^{*}-chemiluminescence is a common technique. The OH^{*}-radical is an intermediate species formed during the oxidation of (fuel-bound) hydrogen to H₂O and hence a good tracer for the flame. For the OH^{*}, the emitted wavelength lies within the Ultra Violet (UV) at 310 nm (± 5 nm). With an optical, narrow band pass filter the light emitted by the radical can be detected. Unfortunately, the light intensity is very small and the sensitivity of the camera's CMOS-chip is rather low at this wavelengths. Therefore, a so-called IRO has been applied in those experiments: Its sensitivity in the UV-range is much higher compared to a CMOS-camera and the amplification makes it possible to detect small numbers of photons. Moreover, since OH^{*} is not the only source of UV light, the setup needed to be extended in order to allow the differentiation between the light coming from OH^{*}-chemiluminescence and the much stronger light coming from the soot incandescence (Figure 10).

Two high speed cameras and one high speed intensifier were necessary to distinguish the two signals: The system produced two pictures which then had to be combined during post-processing. Where UV-signal is present without light at 690 nm, OH^{*} can be detected. As can be seen in Figure 11, the very first image shows a pure OH^{*}-image. One time step later (62.5 μ s), soot is built already at the location where the ignition took place, a larger area ignited and another time step later all these ignited areas again contain soot, as can be seen on the third image.

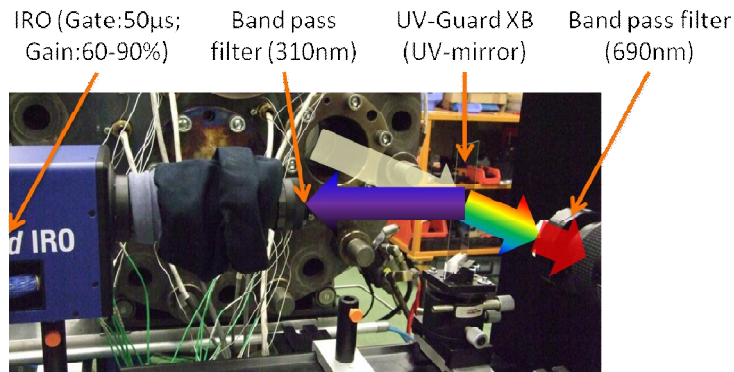


Figure 10: Setup for OH*-chemiluminescence with optical band pass filter, high speed Intensifier and HSS6 to visualize UV-light and Shadow imaging setup to visualize soot incandescence

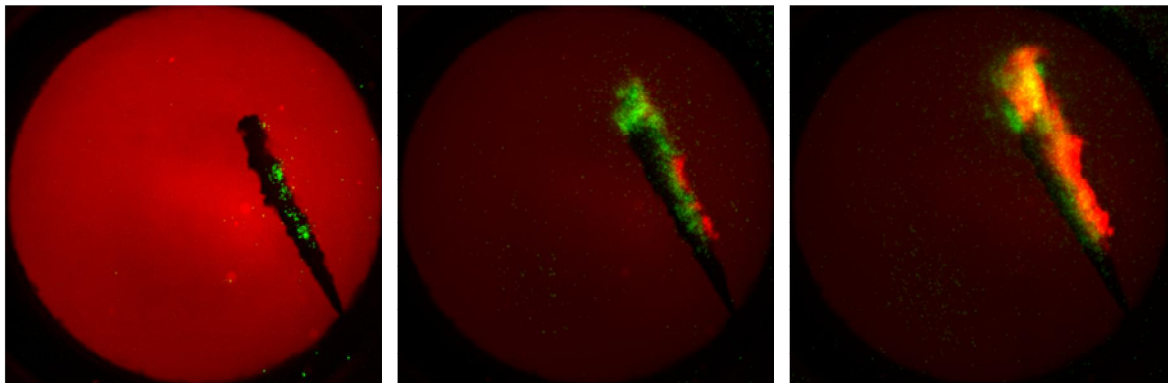


Figure 11: Superposition of UV (310 nm) and visible light (690 nm) signals indicating regions with predominately OH*-chemiluminescence (green) and soot incandescence (yellow/red).

OH* probe application

For the determination of the ignition delay, a fibre optic probe has been used with specific design to detect UV radiation from the OH*-radical. A Kistler sensor, which originally had been designed for in-cylinder investigations of soot formation and oxidation via three colour pyrometry [11], has been used to collect the light emitted by the combustion. The probe coupled the combustion light into a fibre optic cable which transported it to the new optics and amplifying setup shown in Figure 12: The light exits the optical fibre under an angle of $\pm 4^\circ$. A spherical UV-lens is positioned such that the exit of the fibre optic cable lies in its focal point. This distributes the light homogenously across the entire sensitive area of the photomultipliers. In-between, a mirror separates the UV- from the visible light. Light with a wavelength shorter than 370 nm is reflected through a narrow band pass filter. This filter is open for wavelengths of $313 \text{ nm} \pm 5 \text{ nm}$. The visible light passes the low pass filter (UV-mirror) and is sent to a second photomultiplier. The setup so detects the presence of UV-light which can be seen as an indicator for present combustion and helps therefore to investigate the ignition delay.

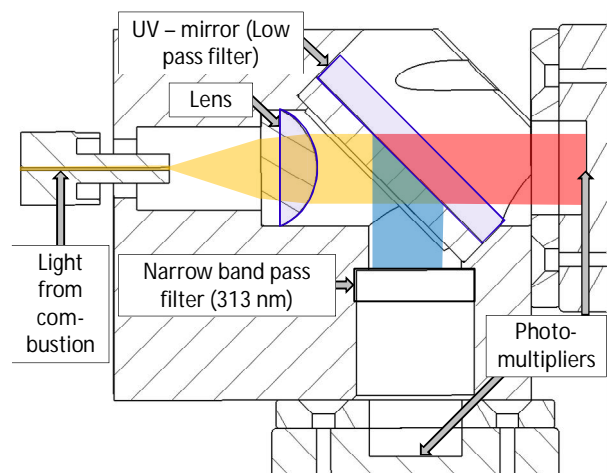


Figure 12: Optical setup to separate and filter the UV-light of 313 nm from the visible light.

Phase Doppler Anemometry (PDA) application

Droplet size and velocity are important information for validating spray models and Phase Doppler Anemometry (PDA) is the technique commonly applied for measuring both quantities. A small measurement volume, consisting of interference layers (=fringes) is produced by crossing two laser beams. If a droplet passes this fringe pattern volume, it scatters light at a certain frequency. Its velocity is proportional to the frequency of the modulation of the scattered light, whereas the size can be determined on the basis of the phase difference of the signal acquired by multiple detectors.

Such PDA system has been installed at the SCC (see Figure 13). In this setup, an Ar-Ion laser is mounted beneath an optical table, whose (green and blue) beams are directed onto the optical table. Via a unique sending optics [12], the beams are then split

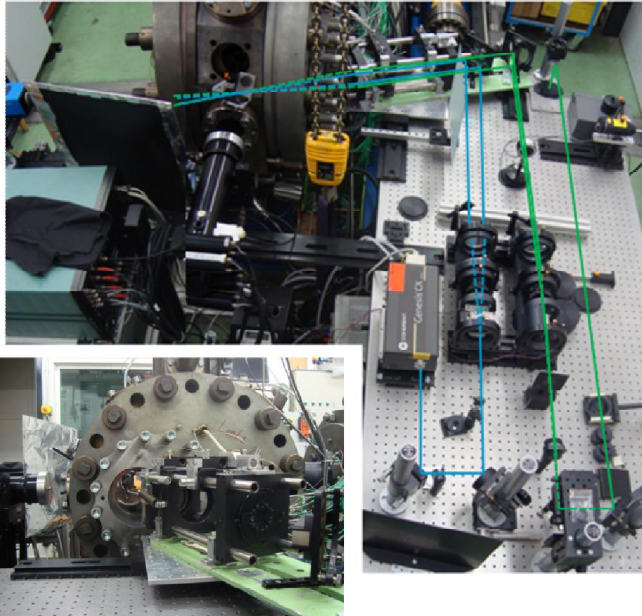


Figure 13: Setup of PDA system at the SCC.

into two beams, each, which are finally crossed inside the chamber in order to generate the 2-D measurement volume. The scattered light signal from the measurement volume is acquired using Dantec receiver optics. An enhanced signal processor is used for initial processing of the acquired data. Further processing is based on customised software from [13] and specifically developed Matlab routines. In order to determine the location of the measurement volume, the shadow imaging setup is used in parallel; however, in correspondence with the lower repetition rate required, the high speed CMOS camera is replaced by a more conventional CCD camera. In 2012, this setup has been upgraded with two custom-made diode-pumped lasers and a new purpose-built beam

alignment setup, which facilitates transport, enhances the robustness and enables the more straightforward use of the system.

Results

The main goal of the Spray Combustion Chamber is the generation of reference data in order to validate new models for describing the behaviour of sprays produced by large marine diesel injectors. In extensive measurement series, a large database comprising measurements related to different aspects of the spray has been produced. The database involves investigations of spray morphology (spray tip penetration, spray angle) for different conditions and fuels. Additionally, it contains measurement data regarding droplet sizes and ignition behaviour. Some of the results have also been presented at different conferences. The CFD experts at Wartsila Switzerland as well as PhD students at ETH Zurich have used different data sets to validate their data and published their results (e.g. [14], [15]).

Phenomenological aspects

A number of systematic measurements for determining the spray evolution and ignition behaviour at various chamber conditions (pressure, temperature) and injection parameters (pressure, spray configurations) using optimized illumination conditions have been performed. In particular, single-spray cases at various orientations of the spray relative to the swirl have been investigated, followed by similar variations for two spray configurations. Additionally, chamber conditions have been varied, specifically considering different pressure levels at high temperature. For the two-spray configurations, also the effect of using non-identical orifice sizes has been studied and finally, a configuration with five (differently-sized) sprays, similar to a typical engine injector design has been employed. Figure 14 exemplary shows image sequences of spray evolution with a two spray configuration at very high temperature conditions (930 K) and three pressure levels (30, 60 and 90 bar) in the spray combustion chamber at start of injection. The well-known dependence of spray behaviour on the density, hence pressure in the chamber at otherwise unchanged conditions is also observed here: With increasing chamber pressure, the penetration is reduced and the spray plumes are becoming wider, specifically close to the spray tips, where it is no longer shielded from the action of the cross-flow by the first spray.

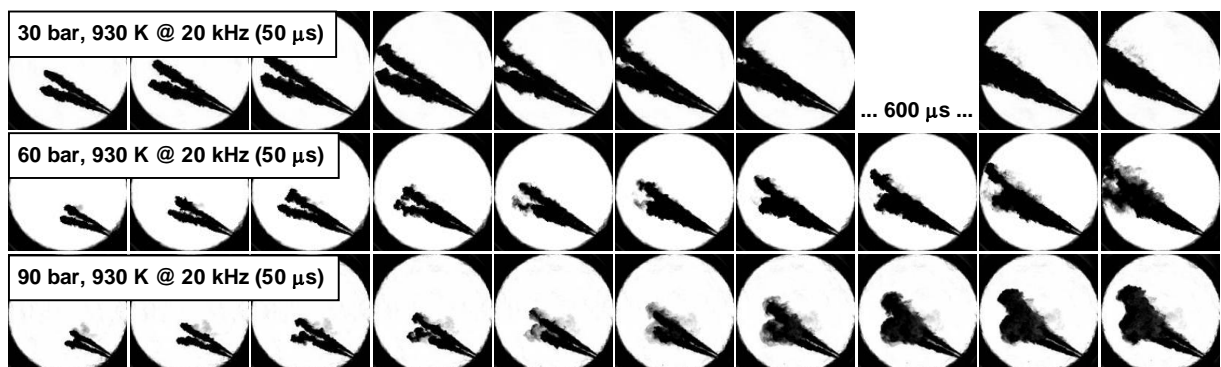


Figure 14: Shadow-images of the temporal spray plume evolution for a two spray configuration at different chamber pressures.

In the high-pressure case, the ignition is occurring within the observation area at a position rather on the lee side of the sprays and combustion is then spreading both towards their tips and the injector. When injecting into a low pressure environment, the ignition takes place considerably later and outside of the visible range and the flames are then propagating back towards the injector.

Reference data generation with light fuel oil (LFO)

An extensive number of systematic inert – by using nitrogen as process gas – investigations for determining the spray evolution at various chamber conditions (p , T) and injection parameters (nozzle tip configuration) have been performed by means of shadow-imaging

measurement campaigns [16]. In particular, the single-hole nozzle cases at various orientations of the spray relative to the swirl have been analyzed in detail in order to obtain initial quantitative reference data with respect to the spray evolution (penetration, angle). Table 1 gives an overview of the major experimental settings with regard to injector (nozzle) and operational parameters (p , T), where all detailed properties (e.g. fuel specifications) can be found in [16]. The single-hole nozzle bore diameter is 0.875 mm in all cases, whereas the nozzle hole exit (defined to be zero perpendicular to the injector axis) is varying from co-axial (90°) to co-swirl (65°), via swirl-perpendicular (50°) to a counter-swirl configuration (40°). The pressure and temperature conditions were kept at 9 MPa / 930 K. For the 50 deg and 90 deg cases pressures of 6 and 3 MPa have also been taken into account. Note that, with identical operation settings, the resulting temperatures are slightly reduced to 920, resp. 900 K. The injection pressure has been set to 1000 bar in order to assure comparable injection behaviour as in marine diesel engine multiple-hole nozzle injection systems.

Hole \varnothing d_0 [mm]	Angle [deg]	Comments	Pressure p [MPa]
0.875	90	Injector co-axial	9/6/3
0.875	65	15° co-swirl	9
0.875	50	Swirl-perpendicular	9/6/3
0.875	40	10° counter-swirl	9

Process gas: Nitrogen (N_2)
Accumulator pressure: 300/180/100 [bar]
Regenerator temperature: 920 [°C]
Intake valve actuating time: 400 [ms]
Swirl flow level: 15 – 25 [m/s]
Combustion chamber temperature: 900 – 930 [K]
Injection pressure: 1000 [bar]

Table 1: Injector nozzle specifications and operation parameter.

Due to the large size of the spray combustion chamber and the practical limitations regarding window size, data from several measurement series have to be superimposed, where the window position was adjusted between series at otherwise unchanged conditions in order to enable the observation of the entire spray evolution, especially at lower pressure conditions. This procedure is exemplarily illustrated already in Figure 5 above, showing a superposition of images obtained at three window positions for one particular set of conditions. The good qualitative agreement of the individual measurements is highlighted when considering the regions where the images from the different measurement series overlap, thus confirming also the high level of reproducibility.

The accurate detection of the spray tip penetration and the cone angles is performed by image processing of the recorded data sets [16]. Figure 15 exemplifies this procedure for the case of a single, injector co-axial spray:

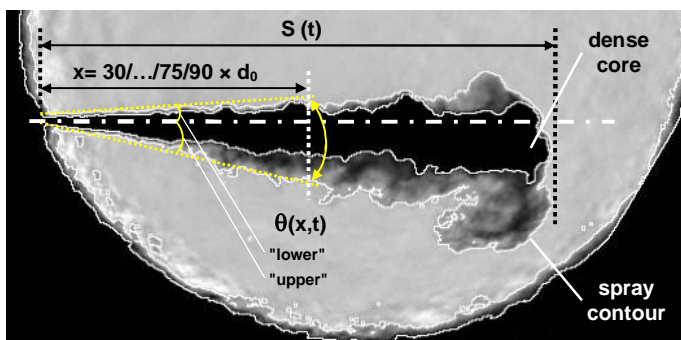


Figure 15: Analysis of spray penetration and cone angles (total, "upper", "lower") on the basis of two spray threshold levels (contour/dense core).

The original image is rotated by 120° in order to horizontally align the axis of the spray. Then, thresholds of 90% (spray contour) and 10% (dense core) of the background gray scale level are applied for determining the spray outlines. The penetration is obtained by measuring the (horizontal) distance from the nozzle tip to the leading edge of the spray – it is worthwhile noting that, in this case, the contours of the spray and its dense core virtually coincide at the spray tip. The identification of cone angle is clearly more difficult – in fact, a variety of such angles could be defined:

Due to the strong swirl, the spray is deflected, resulting in different angles relative to the original axis on the windward ("luv") side of the spray and the side sheltered from the swirl ("lee"). Whereas this effect is virtually negligible for the dense core, it is quite pronounced for the complete spray and we consequently define "lower" (luv side) as well as "upper" (lee side) and total values for the cone angle, which are analyzed at various dis-

tances x/d_0 from the injector tip. In order to account for these special characteristics of the setup, the capabilities of the analysis software employed have been extended accordingly.

Exemplarily, the spray penetration (contour/dense core) of the single-hole injector co-axial nozzle under variation of the chamber pressure (9/6/3 MPa, 930/920/900 K) is shown in Figure 16 (left). As is well-known from earlier investigations at smaller dimensions [18], the spray is propagating linearly along its axis during the initial phase, whereas, in the later propagation stage, its penetration is scaling with the square root of time – hence, the gradient of the curve is decreasing. The spray contour and the dense core are separating at a certain level: Whereas the latter is stabilizing at this (case dependent) level, the spray contour tip continues to propagate and additional effects are becoming relevant (e.g. due to the action of the swirl), such that, for the high pressure case, the gradient is even further decreased during the later injection phase (> 2.5 ms). Reducing the chamber pressure from the above 9 MPa level results in higher injection velocity and therefore faster penetration during the initial phase. The separation of the dense core and the spray contour penetration characteristics mentioned above is exemplarily illustrated in Figure 16 (right). With increasing penetration of the spray, the plume is more and more affected by the acting aerodynamic forces – up to the point, when these are sufficiently high close to the tip of the spray to completely break up the liquid elements of the dense core. After this point, the spray continues to penetrate in the form of the droplet clouds created from the atomisation of the dense core.

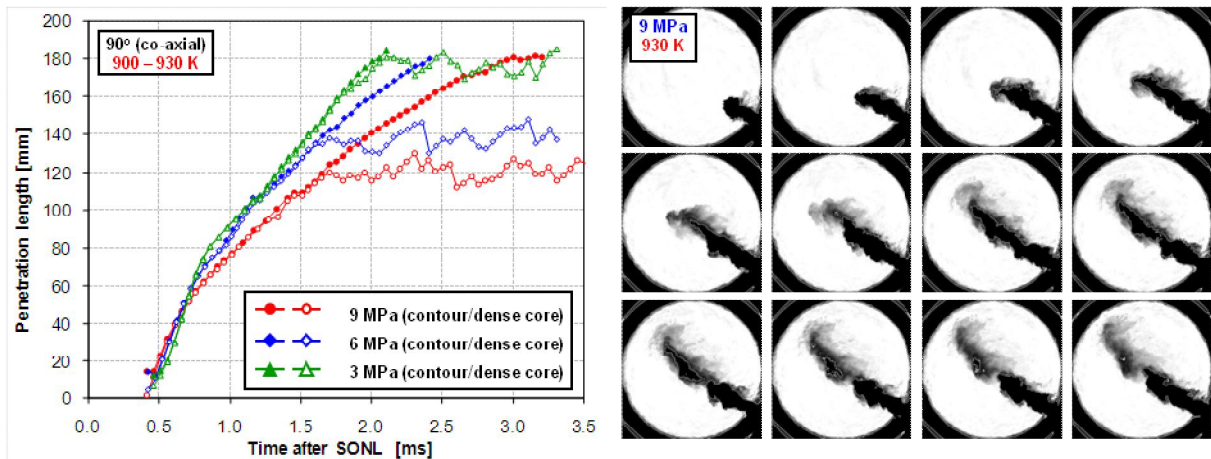


Figure 16: Spray penetration (contour/dense core, left) of the single-hole injector co-axial nozzle at $x/d_0=30$ under variation of the chamber pressure and visualization (right) of the dense core break-up and its fluctuating maximum propagation.

Figure 17 (left) shows a similar analysis for the effect of the orientation of a single-hole nozzle: When moving from a counter-swirl orientation (40°) via swirl-perpendicular (50°) towards co-swirl (65° , 90°) cases, the penetration tends to increase. The swirl influence on the orientation of the spray can be seen in the higher level of the established total cone angle of the 10 deg counter-swirl (40°) compared to the injector co-axial (90°) case at a position of $x/d_0=75$ (Figure 17 right). In addition, also the increasing difference between the spray contour and dense core cone angle levels can be clearly recognized.

Figure 18 (left) shows the behaviour of the two "lower" and "upper" cone angles of the spray contour with respect to the swirl perpendicular (50°) case under a variation of pressure (left) and compared to the injector co-axial case (90° , right). The "upper" (lee side) cone angle is very much affected by the swirl, whereas the "lower" (luv side) cone angle earlier remains at a basically constant, lower level. The deflection of the spray plume under chamber pressure variations (9/6/3 MPa) is recognizable in the upper cone angle as well as in a less pronounced manner in the lower cone angle. The spray orientation influence is displayed in Figure 18 (right), where the counter-swirl case leads obviously to a much larger "upper" (lee side) cone angle of the spray contour than in the co-swirl case, whereas both "lower" cone angles again remain basically constant at a similar, lower level. For the 50° case, also the effect of increasing cone angle with decreasing x/d_0 is recognizable.

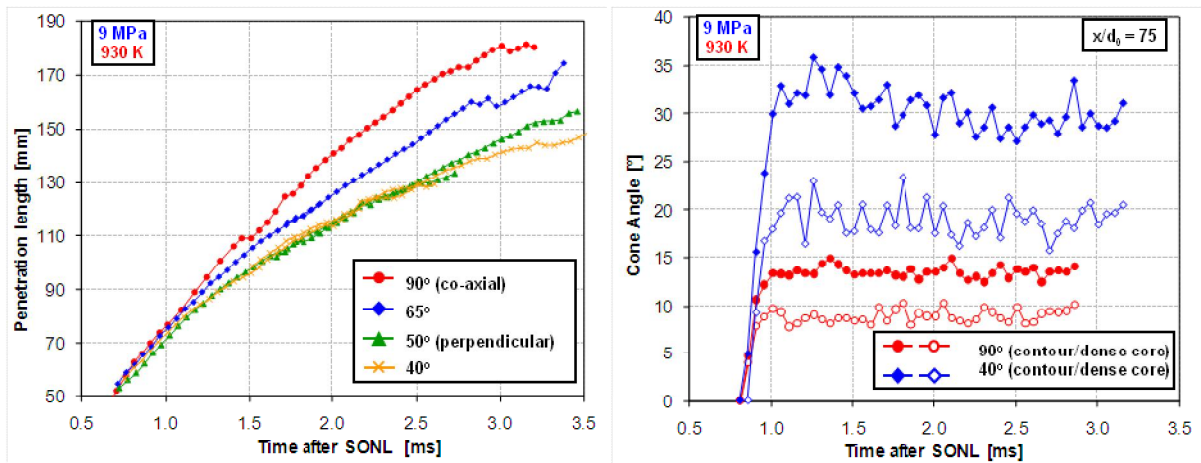


Figure 17: Spray contour penetration of single-hole injectors with different orientation with respect to the swirl (left) and comparison of total cone angles (contour/dense core) of the two most extreme variants at $x/d_0=75$ (right).

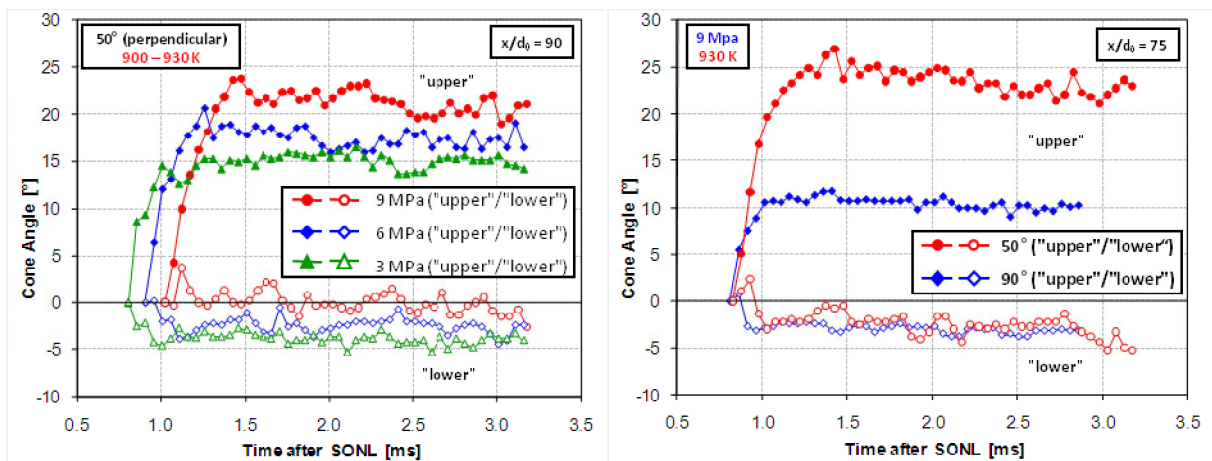


Figure 18: Comparison of "upper" and "lower" cone angles of the swirl-perpendicular case (50 deg) at $x/d_0=90$ for different chamber pressures (left) and compared to the injector co-axial (90 deg) case at $x/d_0=75$ under 9 MPa / 930 K operation conditions.

Figure 19 gives a visual impression of the aerodynamic influence of the swirl with regard to the dense core and the spray contour. The transition region is clearly increased, especially at the lee side compared to the luv side of the spray, and the contour cone angle is increased accordingly as shown above.

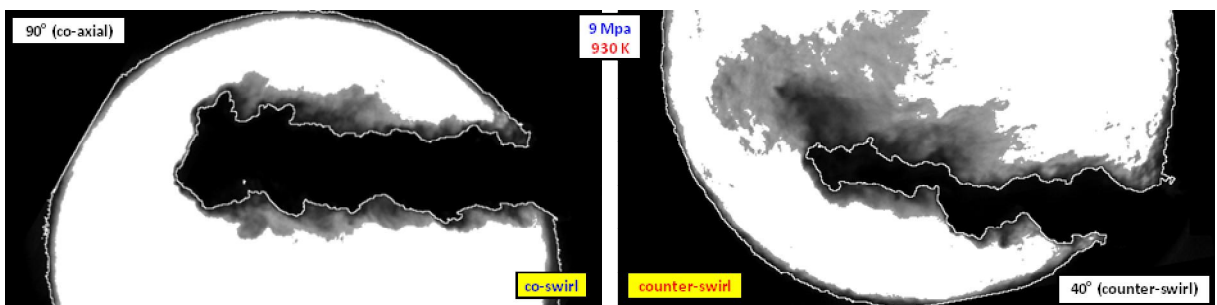


Figure 19: Spray contour and dense core of the injector co-axial case (90 deg) compared to the 10 deg counter-swirl (40 deg) case at 9 MPa / 930 K operation conditions.

Assessment of fuel impact

In the course of extensive measurement series, the influence of fuel properties has been analyzed by comparing the spray propagation of light and heavy fuel oil. Table 2 summarizes the experimental settings regarding the atomizer (nozzle) and operational conditions such as gas density, combustion chamber temperature, swirl, the used process gas (air: reactive; N₂: non-reactive) and the fuel properties of light fuel oil and heavy fuel oil.

Gas density ρ [kg/m ³]	Temp. [K]	Swirl	Process gas	Comments	Properties	Unit	LFO	HFO	Method
33/22/11	900	yes	N ₂	non-reactive	Density at 15°C	kg/m ³	851.4	1001.1	ISO 12185
33/22/11	900	yes	N ₂	non-reactive, HFO	Viscosity at 40°C	mm ² /s	2.928	-	ISO 3104
33/22/11	400	yes	air	non-evaporating	Viscosity at 50°C	mm ² /s	-	1255	ISO 3104
33/22/11	400	no	air	non-evaporating	Gross Heat of Combustion	MJ/kg	45.02	42.74	ASTM D240/D4809
Nozzle hole \varnothing : 0.875 [mm] Nozzle hole angle: 90 [deg] (Injector co-axial) Regenerator temperature: 900/100 [°C] Intake valve actuating time: 400 [ms] Swirl flow level: 15 – 25 [m/s] Chamber temperature: 900/400 [K] Injection pressure: 1000 [bar]					Water Content	% V/V	<0.10	<0.10	ASTM D6304
					Carbon Residue	% m/m	<0.10	17.84	ISO 10370
					Sulphur	% m/m	0.09	0.806	ISO 8754/ASTM D2622
					Ash	% m/m	<0.01	0.018	LP 1001/ISO 6245
					Flash Point	°C	58	103	ISO 2719
					Pour Point	°C	<-6	6	ISO 3016
					Calculated Cetane Index	-	47	-	ISO 4264

Table 2: Summarized experimental settings and operational conditions (left) and fuel specifications (right) of the used light fuel oil (LFO) as well as heavy fuel oil (HFO).

Three different gas densities in the spray combustion chamber have been taken into account (33.7, 21.5 and 11.2 kg/m³) at a constant temperature level of 900 K. The corresponding non-evaporating experiments were performed at the same gas densities but lower temperature (400 K) inside the chamber. Selected results of these experiments have been published in [17].

Figure 20 shows the impact of the fuel quality on the spray parameters (spray penetration, angles) at the various gas density levels. The spray tip penetration of injected light fuel as well as heavy fuel oil is visualized.

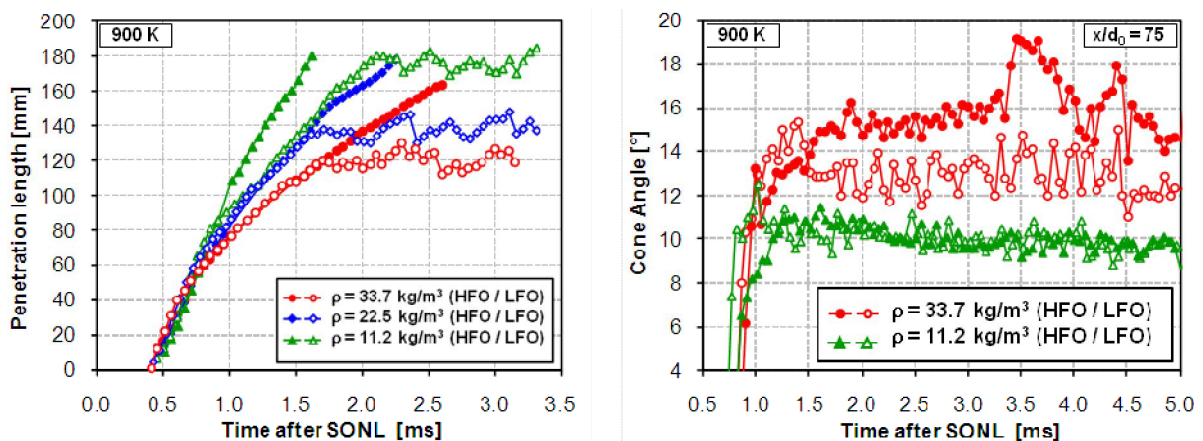


Figure 20: Comparison of light fuel and heavy fuel oil influence on spray tip penetration (dense core) and the cone spray angles (contour) at $x/d_0 = 75$.

The comparison of light fuel and heavy fuel oil sprays injected at evaporating conditions indicates that the fuel properties influence spray evolution and morphology, consistent with earlier investigations using different fuels [19]. The changed fuel composition and properties of the injected fuel have a particular influence on the length of the dense core: At the beginning of the spray propagation, the behaviour of the two fuel types is largely identical. At a later stage of the spray evolution, the dense core of the light fuel oil spray stabilizes at a certain distance. The injected HFO spray, however, is propagating further into the chamber, proba-

bly as a consequence of the differences in key fuel properties such as surface tension, evaporation enthalpy and saturation pressure, which have an impact on the evaporation process and the spray evolution. The corresponding cone angles of the spray reflect the increased influence of the ambient gas density on the spray and the slower evaporation at the spray periphery of the injection with HFO.

Ignition behaviour investigations

The setup for the visualisation of the OH*-radical described above has been used for the investigation of flame lift-off, ignition location and ignition delay of combustion of a marine diesel spray. The outcome of this investigation has been published in [8] and [14], where it has also been used directly as reference data for CFD simulation. Table 3 summarizes the experimental settings regarding the atomizer (nozzle) and operational conditions such as gas density, temperature in the combustion chamber and the fuel properties of light fuel oil.

Gas density ρ [kg/m ³]	Temp. [K]	Swirl [-]	Process gas [-]
33	910	yes	air
33	790	yes	air
33	760	yes	air
33	730	yes	air

Regenerator temperature: **920/790/750/740** [°C]
 Intake valve actuating time: 500 [ms]
 Swirl flow level: 15 – 25 [m/s]
 Nozzle hole angle: 90 [deg] (Injector co-axial)
 Nozzle hole \varnothing : 0.875 [mm]
 Rail pressure: 1000 [bar]

Table 3: Operation parameter and injector nozzle specifications of the experiments.

Figure 21 shows the averaged back illuminated image of a typical spray plume during those tests. As the density was kept constant, the two phase flow was almost identical for all three temperatures. On top of the spray plume the averaged OH*-chemiluminescence images of the flaming areas 125 μ s after ignition (after the first OH* was detected) has been plotted. Together with the individual ignition spots for each measurement – the squares plotted on top of the flaming areas – this provides a good impression of the flame development.

As the ignition delay grows longer with lower temperature, the cloud in which the ignition chemistry is mainly proceeding is transported further downstream such that the ignition location is shifted further away from the nozzle tip. Towards lower gas temperatures, ignition becomes less steady and the location of the ignition spots is more widely distributed. Therefore, the averaged area of the flaming location as well as the area covered by the ignition spots becomes larger. This is, on the one hand, due to the increase in size of the cloud as it is penetrating and mixing further. On the other hand, the high dependency on temperature is playing a role, as small deviations within the temperature distribution along the spray have significant influence on the chemical kinetics and therefore on the location where the ignition starts.

For all cases, the ignition spot is roughly at about half length of spray penetration. With decreased temperature, the location not only moves axially, but also sideways away from the injector axis. Due to the strong swirl, which is typical for large two-stroke engines, the ignition spots are carried to the lee side of the spray plume. The swirl's bending effect on the gas phase is much stronger compared to the liquid phase, as can also be observed in Figure 19. The spray deviates only a few millimetres from the injector axis, whereas the ignition locations lie at a significant distance from the injector and the spray axis.

To allow comparisons at different temperatures the location of the ignition spots has been defined as the axial distance between nozzle orifice and the averaged location of the individual ignition spots (compare the explanation on Figure 21). On the basis of the extensive measurement campaigns accomplished, Figure 22 shows the evaluation of three key parameters measured at four different temperature levels (910/790/760/730 K) inside a reactive spray combustion chamber atmosphere.

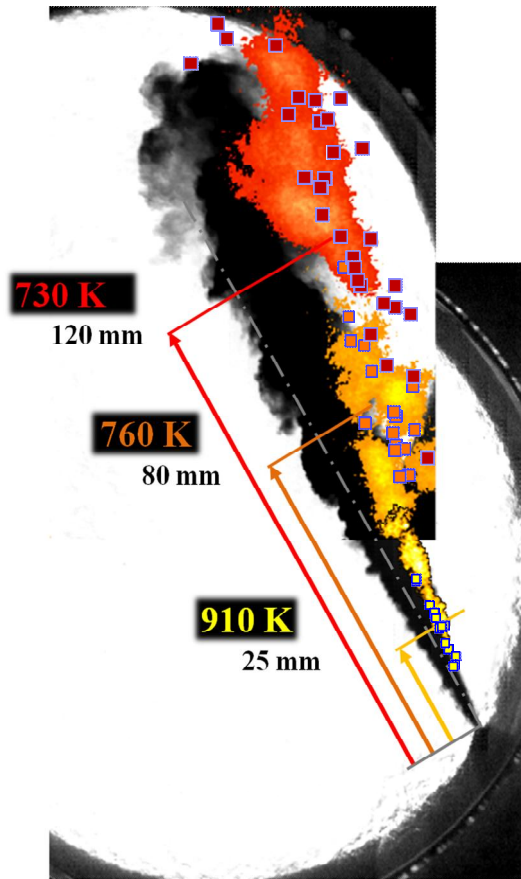


Figure 21: Averaged image of the UV emitting areas 125 μ s after start of combustion for different gas temperatures. The indicated distances represent the distance between the corresponding mean spot and the nozzle orifice

Figure 22 top shows the ignition delay within the observed temperature range. It is defined as the time between start of injection (the moment the first fuel exits the nozzle) and a significant increase in OH* signal in the optical probe. The vertical error bars show the standard deviation, whereas the horizontal bars show the 1% measurement error of the temperature signal. As can easily be seen, the ignition delay grows significantly towards lower gas temperatures.

The main reason for this behaviour is the increased time scale of the chemical processes. Due to the lower temperature, the evaporation process is also slowed down but stoichiometric conditions are still provided. Therefore, the physical processes are not seen as the limiting factor. The mean distances between ignition location and the nozzle tip for all the experiments conducted have been plotted as a function of temperature as visible in Figure 22 bottom. With decreasing temperature, the distance between the orifice and the ignition location is increasing. The slower physical and chemical processes leave more time to the evaporating/evaporated fuel to be transported in axial direction. The fact that the ignition location shows a less distinctive increase towards lower temperature than the ignition delay is consistent with literature, and is associated with the continuous decrease of spray tip velocity. As

The ignition delay between temperatures of 700 K and 810 K was determined by means of an optical fibre probe (compare the corresponding measurement techniques section above) recording a global OH*-chemiluminescence signal. For the first series of experiments at high temperature, the probe was not available, yet; therefore, the ignition delay for these cases has been analyzed via the 2-D OH*-chemiluminescence experiments (This results in an increased temporal uncertainty of 31.25 μ s).

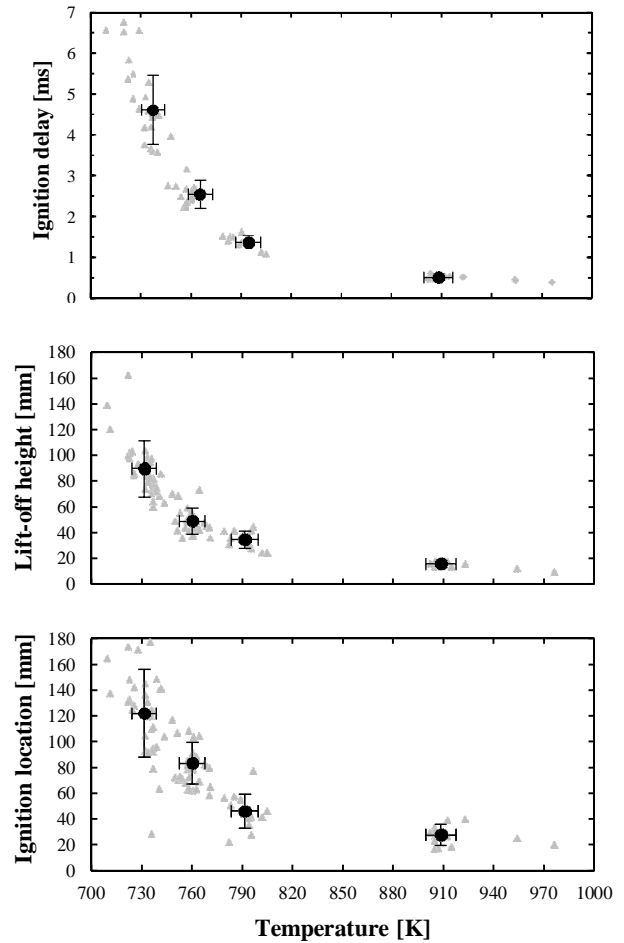


Figure 22: Ignition delay (top), Flame lift-off (middle) and the distance of ignition location (bottom) as function of gas temperature.

can be seen in Figure 21 already, the standard deviation is increased with lower gas temperature. This is mostly due to a higher sensitivity to variations in the temperature distribution of the gas phase. Around 730 K, a difference of 5 K in temperature results in a variation in ignition delay of 1.5 ms. Once the fuel is ignited and the pure-premixed combustion is over, the flame quickly propagates back towards the nozzle until reaching a statistically stabilized minimum distance to the injector, the so called lift-off height. It was defined as the shortest distance in axial direction between the nozzle orifice and the point where OH*-chemiluminescence reached 10% of the maximum intensity. Figure 22 middle shows the lift-off as a function of temperature. Towards lower temperatures the lift-off height increases exponentially. At the same time, the standard deviation increases too; however, in a clearly less pronounced way than for the ignition location.

Determination of droplet size distribution

In a preliminary measurement campaign, the droplet size distribution of the spray has been investigated. The PDA setup has been used on an injection under engine-like density conditions but at low temperatures (non-evaporating case). The conditions for the air in the SCC were 40 bar at a temperature of 400 K. The rail pressure was set to 1000 bar and LFO (light fuel oil) was used as fuel. As nozzle the co-axial type with a nozzle hole diameter of 0.875 mm was installed. The injection duration was set to 10 ms and Laser power was set to 260 mW.

The measurement volume has been positioned as shown in Figure 23 which is about 91 mm downstream or $105 \cdot x/d_0$. The region is not in the dense spray, but in the zone into which

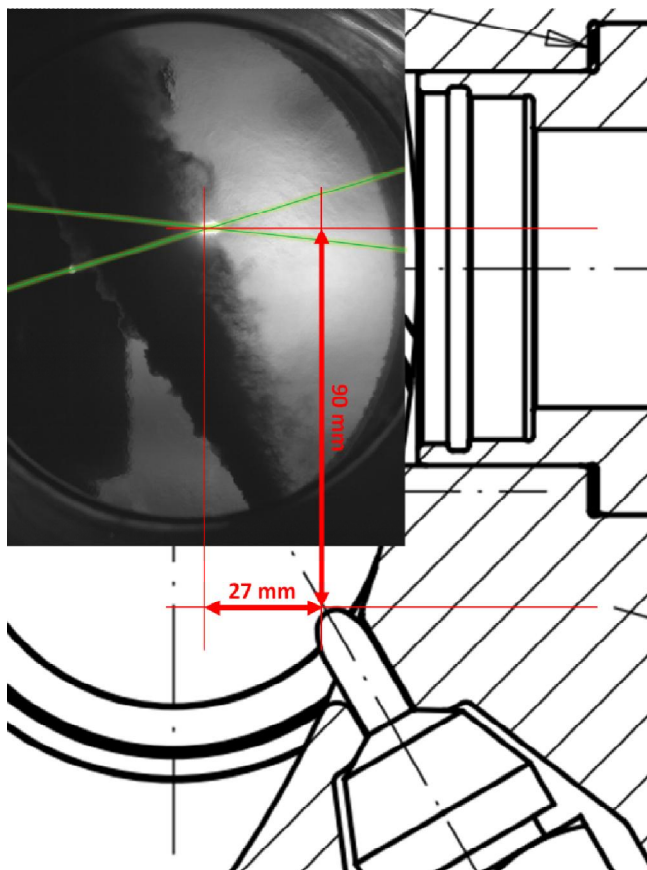


Figure 23: Position of the measurement volume relative to the nozzle tip.

many droplets are deflected by the swirl. This particular selection of measurement volume ensures good accessibility for both the sending and receiving optics. Figure 24 (left) shows the droplet diameters acquired over a series of 40 individual measurements, plotted over their arrival time at the measurement volume after the electronic start of injection. Start and end of injection are clearly recognisable. Due to the distance of the measurement location from the injector, the first signal is delayed with respect to the start of injection. Similar considerations apply at the end of injection; however, some late-comers can be interpreted as signs of non-ideal closing characteristics of the injector.

Figure 24 (right) shows the droplet size distribution, which has a distinct maximum with the largest part of the droplets in the range of about 5 to 35 μm .

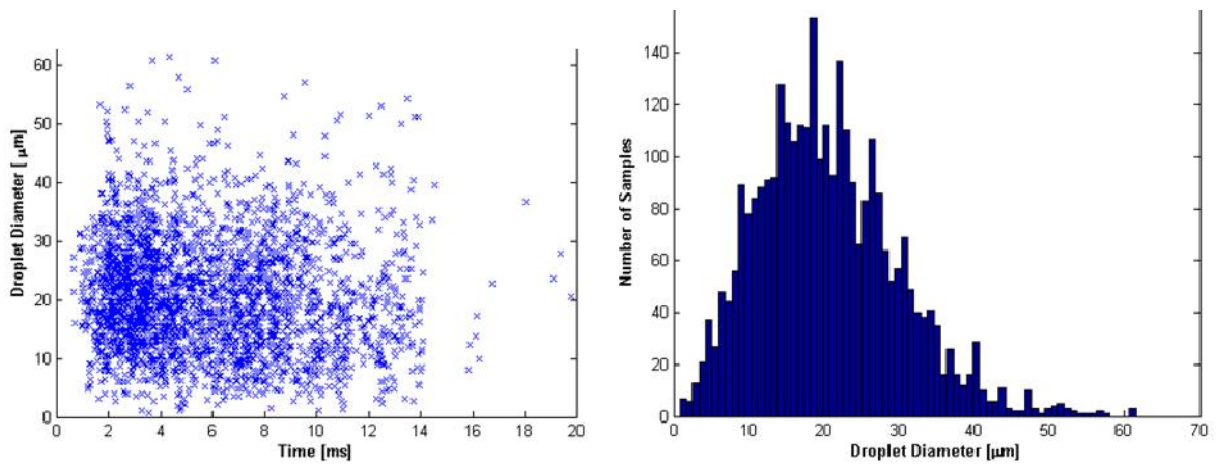


Figure 24: Left: Measured droplet diameters plotted over their arrival time after electronic start of injection, Right: Histogram of the measured droplets.

Extended application: Investigation of lubrication oil injection

The SCC has triggered attention also well beyond its originally intended field of application for the investigation of combustion phenomena in large two-stroke diesel engines. As an example, it has been converted to a test installation for investigating the characteristics of lubrication oil jets, which are employed in most recent engine design for improving the distribution of the lubricant on the circumference of the running surface, compared to traditional, quill-based lubrication systems. This investigation was conducted at considerably lower gas pressure (max. 1 MPa), which allowed the use of less massive covers than those which are used for the reactive experiments (9 MPa; 900 K). A pair of special covers for low pressure experiments was designed, including also the implementation of larger windows with special shapes, which allowed a better observation of the sprays. A very simple design for easy manufacturing and handling was realised and the resulting thin covers were mounted on the SCC using the original bolts in combination with special washers (Figure 25, right image). The rest of the infrastructure (screws, bolts, gaskets, etc) stayed the same.

For the lubrication system experiments, two parallel camera and laser systems were used in order to track the oil injection over its full length via the specifically devised, longitudinally shaped windows. The left side of Figure 25 shows a view from the side of the lasers through the new windows towards the two cam, which were mounted in alignment with the window orientation.

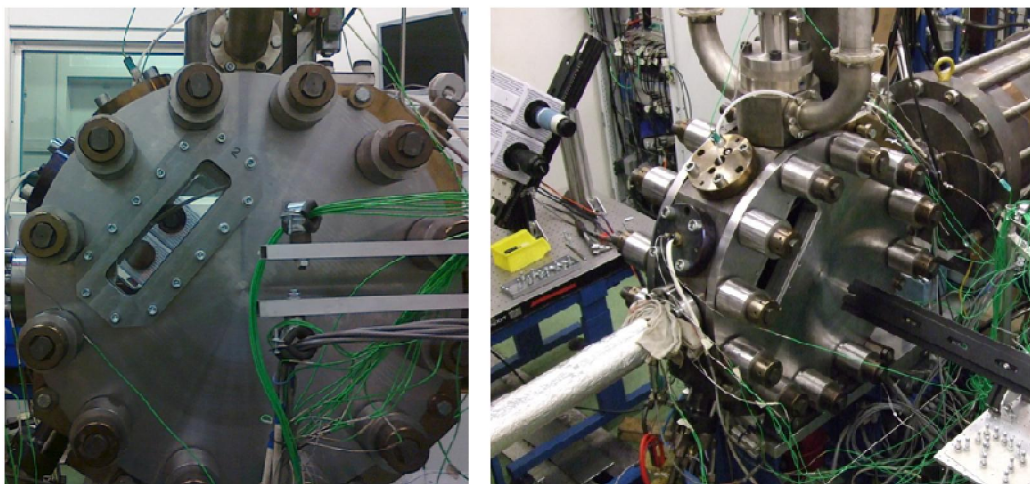


Figure 25: SCC with the new covers and the massive washers to compensate the thickness of the new covers (left). Look through the new window with the two high speed cameras aligned (right).

This work, which has been conducted in collaboration with the Materials & Tribology department of Wartsila Switzerland and the University of Salento, has provided interesting insight into the propagation of lubricant jets at conditions representative of the usual operating regime. An impression of the data obtained is shown in Figure 26. It shows the behaviour of the injected lubricant both for an atmospheric case and a case with 5 bar chamber pressure.

Whereas, in the atmospheric case, the liquid jet is undergoing very basic breakup mechanisms as described in textbooks, its disintegration is much more pronounced in the case at higher pressure and the structure is becoming more similar to a spray as known from the fuel-related investigations on the SCC.

The results of these tests were analysed appropriately in order to define typical parameters characterising the lubricant distribution and its deposition on the running surface (not shown here). These parameters have been the basis for a model, which is now used for investigating options for the further development of the lubricant injection systems and in order to identify optimum specifications for the Wartsila 2-stroke engines.

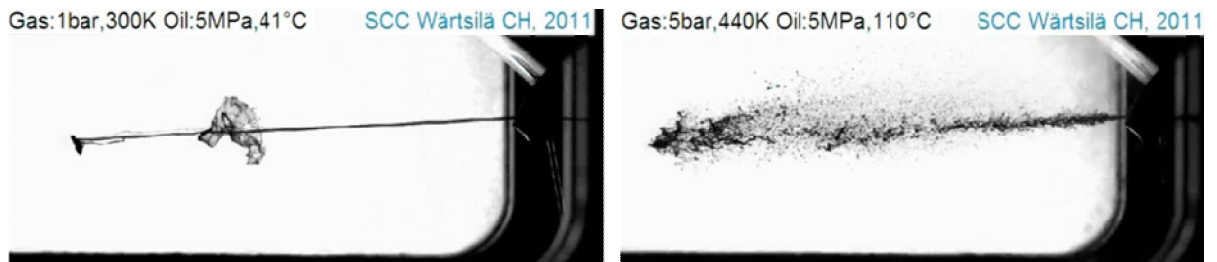


Figure 26: Comparison of lubricant injection visualisations for two oil and gas temperatures.

All in all, this is an excellent example for the versatility of the SCC and how it can be used productively also for investigations beyond the original scope of application.

Conclusions and Outlook

In the course of the past 4 years, the Spray Combustion Chamber has been fully commissioned, validated, further improved as well as extended and subsequently used for a large variety of measurement series. This has involved both the extension of the range of measurement techniques applied and the further development of the SCC for increased variability and higher operational efficiency.

As regards the latter, major steps have been achieved by realising the enhancement of the optical accessibility and implementing the additional fuel injection system for heavy fuel oil. In addition, the capability of the setup for assessing the performance of actual engine injector configurations could be successfully demonstrated. A next important step will be the commissioning of the media separator in order to further enhance the flexibility in terms of the investigation of different fuels.

After first measurements of the spray plume evolution and ignition behaviour by means of shadow-imaging measurements, a large number of systematic measurement campaigns at non-reactive conditions were performed. The systematic analysis of the acquired data has produced an initial set of spray propagation reference data, consisting in relevant characteristics such as penetration and spray angles for a whole range of conditions. The variations considered include the most important parameters for (single) light fuel oil sprays such as chamber pressure and temperature, injector orifice size, spray orientation with respect to the swirl, swirl intensity or injection pressure. As a consequence, we now dispose of a comprehensive reference data set, which is already extensively used for the validation of CFD modelling approaches.

This reference data set has been extended by performing a series of measurements on heavy fuel oil, both for reactive and non reactive conditions. These investigations confirmed for instance that HFO sprays exhibit significantly different behaviour compared to their light fuel counterparts under evaporating (but non reactive conditions): It takes the spray much longer to evaporate and, therefore, the liquid core penetrates considerably further into the combustion chamber. The influence of fuel properties on the spray angle becomes relevant for higher gas densities; where the spray angle of HFO is increased compared to LFO. However, the experiments conducted so far also give rise to further questions and the behaviour of HFO sprays is not yet fully understood. Therefore, further investigations are necessary, including additional fuel types.

The next important step in complementing the know-how on fuel sprays will be the realisation of a comprehensive test series with Phase Doppler Anemometry in order to determine drop-size and velocity data. The work envisaged involves both fundamental investigations into the applicability to and characterisation of the measurement technology for HFO and the actual tests on the SCC, thereby building upon the successful pre-tests performed as part of the present project.

The applicability of OH^{*}-chemiluminescence for investigating ignition and combustion processes of a marine diesel sprays has also already been demonstrated. This study will be extended accordingly in order to cover all key parameters, including the effect of fuel quality. In order to obtain a yet better understanding of combustion phenomena, the application of more advanced measurement techniques will have to be considered.

Another focus area of future work is the investigation of the flow inside the injector and its impact on spray behaviour and combustion, in accordance with the targets of the HERCULES-C project [5], which started in January 2012. In particular, different geometrical configurations of injectors will be tested in order to establish correlations of the main parameters of such designs and key spray characteristics. This may also involve the introduction of new measurement technologies for assessing the injector performance in more detail and for observing the behaviour of sprays in the primary breakup region close to the injector orifice.

All in all, the Spray Combustion Chamber has clearly demonstrated its value: It has proven its robustness and can be operated at high levels of reliability, which has even been further increased by building in redundancy in various subsystems. It allows generating data, which are characterised by outstanding reproducibility and very high quality. The data processing,

which has been put in place, enables the fast and efficient analysis of the raw data obtained in order to derive relevant scientific conclusions. Its unique features and high versatility – as has for instance been demonstrated in the application for the investigation of lubricant oil injection – make it a very powerful and invaluable tool both for fundamental research into spray and combustion processes and for enhancing product development by assessing the performance of new components and systems that can be applied to it.

National Collaboration

On the national level, two other major partners are directly involved: The "Aerothermochemistry and Combustion Systems Laboratory" (LAV) [20] of ETH Zurich and the Combustion Research Laboratory (CRL) [21] of the Paul Scherrer Institute (PSI). Both are partners within the "Workpackage 2 (WP-2), Advanced Combustion Concepts", "Task 2.1, Combustion Process Simulation" of the HERCULES-B project (2008-2011) as well as in "Workpackage 3 (WP3), Injection, Spray Formation and Combustion" of the HERCULES-C project (since 2012).

The "Aerothermochemistry and Combustion Systems Laboratory" (ACL) has been a main contributor to the development of the spray combustion chamber test facility. Today, its collaboration now is more on the simulation side in order to test, validate and improve models based on the reference data provided. The collaboration with the "Combustion Research Laboratory" at PSI is based on the expertise in measurement techniques available and the earlier cooperation in this area.

Beyond this formal collaboration, there is also close cooperation with the "Laboratory Internal Combustion Engines" of EMPA [22], specifically with respect to the application of the PDA system, which is used jointly by the LAV, EMPA and Wärtsilä teams.

The close contact and continuous exchange of experience and know-how and the use of synergies, specifically related to the application of measurement technology and infrastructure, proves to be of constant benefit for all partners.

International Collaboration

On the international side, the collaboration is also taking place mainly within the HERCULES series of projects in the context of EU's Seventh Framework Programme (fp7). These projects are aiming at the development of a future generation of optimally efficient and clean marine diesel power plants. They are the outcome of a joint vision by the two major European engine manufacturer groups, Wärtsilä and MAN Diesel & Turbo, which together hold 90% of the world's marine engine market. The overall research objectives focus on the drastic reduction of CO₂ emissions from maritime transport, and aim at achieving near-zero emissions, thereby maintaining the technical performance of engines throughout their operational lifetime.

The total consortium consists of 32 (HERCULES-B), respectively 22 (HERCULES-C) partners, covering all sectors of marine engine technology: engine manufacturers, suppliers, universities and research organisations, classification societies as well as end-users. In general, there is strong interest in the development and application of simulation methods and tools and, consequently, also in the results of experimental investigations such as conducted on the SCC for model validation.

Outside of HERCULES, there is an informal exchange with other universities or institutions active in similar fields.

The investigation of lubrication oil injection has been conducted in collaboration with the "Department of Engineering for Innovation" of the University of Salento, Italy [23].

References

- [1] I.P. HERCULES, Contract No: TIP3-CT-2003-506676, Deliverable: D2.1.c, Experimental characterization of fuel spray, mixing and combustion processes in marine engines, 2007.
- [2] <http://www.ip-hercules.com>
- [3] SOFE, BFE Projekt-Nr. 100706 / Verfügungs-Nr. 150822, Annual Reports, 2004-2007.
- [4] <http://www.hercules-b.com>
- [5] <http://www.hercules-c.com/>
- [6] K. Herrmann, A. Kyrtatos, R. Schulz, G. Weisser (Wärtsilä Switzerland Ltd), B. von Rotz, B. Schneider, K. Boulouchos (ETH Zurich), Validation and Initial Application of a Novel Spray Combustion Chamber Representative of Large Two-Stroke Diesel Engine Combustion Systems, ICLASS 2009, 11th Triennial International Annual Conference on Liquid Atomization and Spray Systems, Vail, Colorado USA, July 2009.
- [7] S. Semadeni, R. Schulz, Wärtsilä Switzerland Ltd, Internal Report 2004
- [8] Andreas Schmid, Beat von Rotz (Wärtsilä Switzerland Ltd.), Rolf Bombach (Paul Scherrer Institute), et. al. Investigation of Marine Diesel Ignition and Combustion at Engine-Like Conditions by means of OH* Chemiluminescence and Soot Incandescence, COMODIA2012, 8th International Conference on Modeling and Diagnostics for Advanced Engine Systems, Paper CI-8, Fukuoka, Japan, July 2012
- [9] <http://www.lavision.de/en/techniques/shadowgraphy.php>
- [10] B. Schneider, Experimentelle Untersuchung zur Spraystruktur in transienten, verdampfenden und nicht verdampfenden Brennstoffstrahlen unter Hochdruck, PhD thesis, No. 15004, ETH Zürich, 2003.
- [11] KTI-Projekt 10604, Schlussbericht, Vögelin Ph., Bertola A., Obrecht P., Boulouchos K. 2011
- [12] Wigley G., Hargrave G.K., Heath J., "A High Power, High Resolution LDA/PDA System Applied to Dense Gasoline Sprays", 9th Int. Symposium on Applications of Laser Techniques to Fluid Mechanics, Lisbon, 1998
- [13] Schneider, B. (1999 - 2012). PDA Grapher (Software for PDA Data analysis). Zürich, Switzerland.
- [14] Michele Bolla, Yuri M. Wright and Kostantinos Boulouchos (ETH Zurich). Application of a Conditional Moment Closure Combustion model to a large two-stroke marine Diesel engine reference experiment, COMODIA2012, 8th International Conference on Modeling and Diagnostics for Advanced Engine Systems, Paper MS3-2, Fukuoka, Japan, July 2012
- [15] S. Hensel, K. Herrmann, R. Schulz, G. Weisser: „Numerical analysis and statistical description of the primary breakup in fuel nozzles of large two stroke engines for the application in CFD engine simulations“, “COMODIA 2012: 8th International Conference on Modeling and Diagnostics for Advanced Engine Systems“, Fukuoka, 2012
- [16] K. Herrmann, B. von Rotz, R. Schulz, G. Weisser, K. Boulouchos and B. Schneider, Reference Data Generation of Spray Characteristics in Relation to Large 2-Stroke Marine Diesel Engines Using a Novel Spray Combustion Chamber Concept, ICLASS 2010,

23rd Annual Conference on Liquid Atomization and Spray Systems, Brno, Czech Republic, September 2010.

- [17] B. von Rotz, K. Herrmann, G. Weisser, M. Cattin, M. Bolla and K. Boulouchos, Impact of Evaporation, Swirl and Fuel Quality on the Characteristics of Sprays typical of Large 2-Stroke Marine Diesel Engine Combustion Systems, 24th ILASS Conference, Estoril 2011
- [18] H. Hiroyasu, M. Arai, Structures of Fuel Sprays in Diesel Engines, SAE 900475, 1990.
- [19] Higgins B.S., Mueller C.J., and Siebers D.L. SAE 1999-01-0519 (1999).
- [20] <http://www.lav.ethz.ch>
- [21] <http://crl.web.psi.ch/>
- [22] <http://www.empa.ch/>
- [23] <http://www.dii.unisalento.it/>